



Spatially explicit modelling of transgenic maize pollen dispersal and cross-pollination

Christine Loos^a, Ralf Seppelt^{a,*}, Sara Meier-Bethke^b, Joachim Schiemann^b, Otto Richter^a

^a *Department of Environmental System Analysis, Institute of Geoecology, Technical University of Braunschweig, Langer Kamp 19c, 38106 Braunschweig, Germany*

^b *Federal Biological Research Centre for Agriculture and Forestry, Institute for Plant Virology, Microbiology and Biosafety, Messeweg 11/12, 38104 Braunschweig, Germany*

Received 17 December 2002; received in revised form 5 June 2003; accepted 11 June 2003

Abstract

Modelling of pollen dispersal and cross-pollination is of great importance for the ongoing discussion on thresholds for the adventitious presence of genetically modified material in food and feed. Two different modelling approaches for pollen dispersal are used to simulate the cross-pollination rate of pollen emerged from an adjacent transgenic crop field. The models are applied to cross-pollination data from field experiments with transgenic maize (*Zea mays*). The data were generated by an experimental setup specifically designed to suit the demands of mathematical modelling. First a Gaussian plume model is used for the simulation of pollen transport in and from plant canopies. This is a semiempirical approach combining the atmospheric diffusion equation and Lagrangian methodology. The second model is derived from the localised near field (LNF) theory and based on the physical processes in the canopy.

Both modelling approaches prove to be appropriate for the simulation of the cross-pollination rates at distances of about 7.5 m and more from the transgene source. The simulation of the cross-pollination rate is less precise at the edge of the source plot especially with the LNF theory. However, the simulation results lie within the range of variability of the observations. Concluding can be pointed out that both models might be adapted to other pollen dispersal experiments of different crops and plot sizes.

© 2003 Elsevier Ltd. All rights reserved.

Keywords: GMO; Pollen dispersal; Cross-pollination; Gaussian plume model; Micrometeorology; Localised near field theory

1. Introduction

In the European Union rules are put in place on the labelling of foodstuffs to enable European consumers to get comprehensive information on the contents and the composition of food products including genetic modification. Labelling helps consumers to make an informed choice while purchasing their foodstuffs. A threshold of 1% was established for the adventitious presence of (authorised) genetically modified (GM) material in food and food ingredients in respect of labelling under Commission Regulation No 49/2000. Threshold values for technologically unavoidable and coincidental additions of raw material of genetically modified organisms (GMOs) are discussed for agricultural

products (DFG Senate commission, 2001). For food and animal feed a threshold value of 1% and for seed phased threshold values of 0%, 0.3%, 0.5% and 0.7% are under discussion (DFG Senate commission, 2001). The observance of threshold values requires information on pollen spread from GM crops to neighbouring conventional crops and on subsequent cross-pollination rates to related species. The most important factor controlling cross-pollination is the dispersal distance pollen can cover. For this reason the main focus in this study is to quantify the pollen dispersal from GM crops and the subsequent cross-pollination to related species.

Published data on pollen dispersal experiments show that a comparison between dispersal data of different field experiments is hardly possible (Emberlin et al., 1999; Treu and Emberlin, 2000; Lavigne et al., 1998). Limitations are due to the strong dependence on the shape and extent of the source and receptor plot and

*Corresponding author. Tel.: +49-531-391-5608; fax: +49-531-391-8170.

E-mail address: r.seppelt@tu-braunschweig.de (R. Seppelt).

Nomenclature			
C_d	effective drag coefficient	z_0	roughness length (m)
d	deposition coefficient	z_s	source height (m)
d_0	zero-plane displacement height (m)	Δz	difference between source and receptor height (m)
f_w	coefficient for description of wind direction	<i>Greek letters</i>	
h	average height of maize plants (m)	σ	standard deviation from mean wind direction (deg)
o	orientation of sampling array (deg)	σ_w	Eulerian vertical velocity standard deviation (m s^{-1})
p_1, p_2	coefficients for description of source term	ζ	dimensionless distance
P	transition probability density (m^{-3})	ω	mean wind direction (deg)
T_L	Lagrangian time-scale (s)	<i>Other symbols</i>	
t	time (s)	-	average value
u	wind velocity (m s^{-1})	'	deviation from average
u_*	friction velocity (m s^{-1})		
w	weighting factor for wind direction		
x_j	coordinates (m)		
z	height (m)		

particularly the strong influence of different weather situations even if the same crop is used (Lavigne et al., 1998). For this reason a considerable requirement for research on mathematical models for the simulation of pollen dispersal can be identified.

The major aim of this study is to apply and to compare different modelling approaches for pollen dispersal and the resulting cross-pollination to a field experiment with transgenic maize (*Zea mays*). From these, general dispersal patterns of maize pollen are derived, which are important for risk assessment and management strategies of GM crops and provide a basis for the ongoing discussion on thresholds for the adventitious presence of GM material in food and feed.

2. Maize pollen dispersal

2.1. Biology and system analysis

Maize is diclinous, e.g. male flower and the female flower are at different spatial location of the crop. For this reason, insect borne pollen transport leading to cross-pollination can be neglected and maize is an ideal organism for studying and modelling pollen dispersal driven by wind borne pollen transport. Nevertheless, the environmental and biological processes are complex. In general the pollen are shed from the tassel, the male flower at the top of the plant, before the female flower, the ear with the silk, is receptive, but a small overlap is also possible. This can be seen in the fact that up to 5% of the pollination of maize is due to self-pollination (Emberlin et al., 1999). For an anemophilous species the maize pollen is very large with a grain size of 90–125 μm and a weight of about 247×10^{-9} g. As a result, the pollen grains have a high terminal velocity of 20 cm s^{-1} ,

a settling velocity of 40 cm s^{-1} and a deposition coefficient (d) of 0.20 (Emberlin et al., 1999). In normal weather conditions the pollen remains viable for about 24 h, hot weather can reduce this time to a few hours, cool and humid conditions can extend this viability to several days.

2.2. Experimental setup

Cross-pollination data of a monitoring farm scale experiment carried out at the Federal Biological Research Centre for Agriculture and Forestry (BBA) in Braunschweig, Germany were used for model application and verification (Meier-Bethke and Schiemann, 2002). The model predictions were compared against measured cross-pollination rates in conventionally bred maize in distances up to 50 m around a source plot (GM maize) of a size of 1 ha (100 m \times 100 m). Around the GM maize plot a maize-free strip of about 2 m was established. The field trial was carried out with a herbicide-resistant line of maize. The surrounding seed consisted of ordinary maize of the same variety. The maize was planted in rows at intervals of 0.75 m with a distance of about 0.16 m between the single plants.

The plants grew to an average height of 2.45 m with a tassel length of about 30 cm, so that most of the pollen was emitted at heights of about 2.30–2.60 m. The corn ear was located in the middle at 0.85 m. Pollen emission and pollination time varied between single areas in the field, although exact time data of pollen emission are not available. On average the pollination season of the plot was from 14 July to 11 August 2000. During the pollination season the prevailing wind was coming from the north-west.

The source plot was surrounded by 16 sampling arrays in equally spaced distances that is sampling

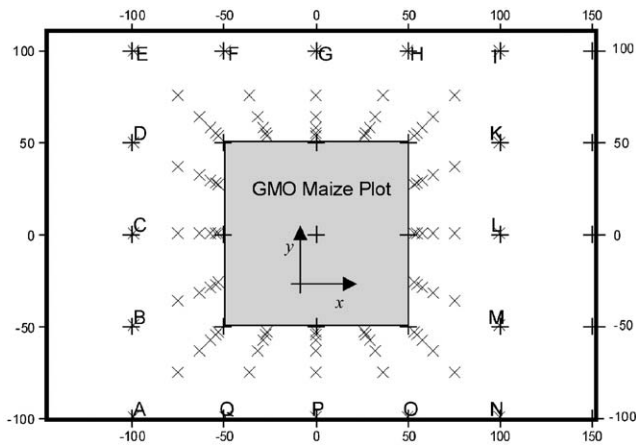


Fig. 1. Spatial geometry of field experiment carried out in 2000 by the Federal Biological Research Centre for Agriculture and Forestry (BBA). In the centre the 1 ha plot with transgenic maize is located within a field with ordinary maize of the same variety. The crosses specify the locations of sampling sites. The transects are specified by capital letters A to Q.

positions spaced at 22.5° intervals. Each array was composed of six sampling points in distances of 3, 4.5, 7.5, 13.5, 25.5 and 49.5 m distance from the edge of the source. Fig. 1 displays a map with the spatial experimental design. At every sampling point a defined amount of corn grains (at least 60 cobs) were sampled, and a sub-sample of 1.5 kg was analysed by a so-called germination test, performed at BBA (Meier-Bethke and Schiemann, 2000). The maize grains were germinated in the greenhouse, after 10 days the seedlings were treated with the herbicide Glufosinate and after 3 weeks the test was completed. The seedlings, which survived the treatment, were identified as genetically modified so that they showed herbicide resistance. By this process the amount of genetically modified maize seeds can be counted and the cross-pollination percentage is calculated. A minimum of 2497 maize kernels up to 4996 maize kernels were examined per sample to allow valid statements for outcrossing rates above 0.5%.

3. Modelling pollen dispersal

3.1. Application of atmospheric diffusion theories for pollen dispersal modelling

A common way to describe the transport of scalars in an open environment is the atmospheric diffusion equation. In the atmospheric diffusion equation the mean concentration $C(x, y, z)$ of particles is expressed by a solution of the advective conservation equation with gradient-diffusion theory (Katul and Albertson, 1999; Van den Hurk and McNaughton, 1995; Seinfeld and Pandis, 1998). When pollen are observed it can be

assumed that molecular diffusion is negligible compared with turbulent diffusion. Employing the gradient-diffusion theory the mass-conservation equation becomes

$$\frac{\partial C}{\partial t} + \bar{u}_j \frac{\partial C}{\partial x_j} = \frac{\partial}{\partial x_j} \left(K_{jj} \frac{\partial C}{\partial x_j} \right) + S(x, t) \quad \text{for } j = 1, 2, 3 \quad (1)$$

assuming an incompressible atmosphere with the eddy diffusivity K_{jj} and the deterministic part of the wind velocity \bar{u}_j . S is a source or sink distribution at location $\mathbf{x} = (x, y, z)$ and time t . The basis for a large class of atmospheric diffusion formulas describing stationary, homogeneous turbulence is the fact that the mean concentration emitted from a point source has the form of a Gaussian distribution (Seinfeld and Pandis, 1998). An approach based on these principles is called a *Gaussian plume model*.

Transfer in canopies has to be treated differently to that in the free atmosphere, for which the gradient-diffusion theory is widely used. Attempts to apply the gradient-diffusion theory to plant canopies identified the problem of counter-gradient fluxes. The reason for the failure of the theory is the coherent character of the turbulence statistics in plant surfaces and that the vertical scalar transfer is maintained by eddies with length scales of the order of the canopy height h (Raupach, 1987).

Efforts to circumvent the limitation of gradient-diffusion theory resulted in two main approaches in micrometeorological modelling: Lagrangian dispersion models (Raupach, 1987, 1989a, b; Van den Hurk and McNaughton, 1995; Baldocchi, 1997; Katul et al., 1997; Massman, 1999; Gu et al., 1999; Warland, 1999) and higher-order Eulerian closure models (Wilson and Shaw, 1977; Meyers and Paw, 1986; Katul and Albertson, 1999).

In the *Localised near field (LNF) theory* proposed by Raupach (1989a, b) the concentration profiles of scalars within plant canopies are predicted by a Lagrangian dispersion model. As in previous works (Van den Hurk and McNaughton, 1995; Katul et al., 1997; Massman, 1999) the LNF theory has often been used to predict the concentration profiles of CO_2 , heat and water vapour, the approach is scarcely used for the prediction of the transfer of pollen and spores in canopies. The objective of this work is to examine whether a Gaussian plume model or the LNF theory are capable for the simulation of pollen dispersal.

3.2. Gaussian plume model

With the Gaussian plume model the atmospheric diffusion equation (1) is solved analytically in dependence of the source distribution. For an instantaneous point source of strength S we refer to the solution presented by Seinfeld and Pandis (1998). Assuming flow in the x and y direction with a velocity u_x and u_y and

constant K_{xx} , K_{yy} and K_{zz} , the mean concentration can be expressed by

$$C(x, y, z, t) = \frac{S}{2\sqrt{2(\pi t)^3(K_{xx}K_{yy}K_{zz})}} \times \exp\left(-\frac{(x-u_x t)^2}{4K_{xx}t} - \frac{(y-u_y t)^2}{4K_{yy}t} - \frac{z^2}{4K_{zz}t}\right). \quad (2)$$

This equation shows that the mean concentration resulting from an instantaneous point source has a distribution that is Gaussian. Data on cross-pollination from field experiments indicates that the pollen dispersal shows a characteristic distribution in the area near the GM maize field with high rates of cross-pollination and in the area further away from the field with smaller rates. This observation leads to the supposition that the pollen distribution of a single maize plant C_{plant} can be given by a superposition of two Gaussian distributions with different eddy diffusivities. It is assumed that the turbulent diffusion process is independent on direction and that the eddy diffusivities for the x , y and z direction are equal ($K_{xx} = K_{yy} = K_{zz}$).

$$C_{plant} = \alpha_w C(x, y, z, t, K_1) + (1 - \alpha_w) C(x, y, z, t, K_2), \quad (3)$$

where K_1 is the eddy diffusivity for the near-distribution of pollen, K_2 for the far-distribution and α_w a weighting factor between 0 and 1, refer to nomenclature for an overview of defined variables and parameters.

The Lagrangian principle is used to specify the distribution for all maize plants in the field. The transition probability density function can be supposed as the probability that a pollen grain from plant located at $\mathbf{x}_0 = (x_0, y_0)$ pollinates plant at $x = (x, y)$ and is therefore the probability of cross-pollination. The total amount of pollen received by a plant can be expressed as the sum of pollen it receives from every plant in the field (Lavigne et al., 1998).

$$C_{field}(x, y, \Delta z, t) = \int_{-\infty}^{\infty} \int_{-\infty}^{\infty} C_{plant}(x - x_0, y - y_0, \Delta z, t) g(x_0, y_0) dx_0 dy_0 \quad (4)$$

with C_{field} being the total amount of pollen a plant receives from a specified part of the field and C_{plant} the pollen probability distribution of a single plant with source strength S . $g(x_0, y_0)$ is the unit source strength since the plants are assumed to coincide in flowering and all produce the same amount of pollen. The difference in elevation between the source z_0 (tassels of the maize plants) and the receptor z (ears with silks of the maize plants) is constituted on the constant difference Δz . This resulting model can be interpreted as a transfer-function, translating spatially explicit pollen distribution to cross-pollination. This transfer-function incorporates

the processes of dispersal, deposition and transport in an aggregated way.

3.3. Localised near-field theory model

3.3.1. Basic assumptions

In the Lagrangian approach, the mean concentration of a scalar $C(\mathbf{x}, t)$ is related to the statistics of the ensemble of marked fluid particles by the transition probability density function $P(\mathbf{x}, t | \mathbf{x}_0, t_0)$.

$$C(\mathbf{x}, t) = \int \int_{R^3} \int_0^t P(\mathbf{x}, t | \mathbf{x}_0, t_0) S(\mathbf{x}_0, t_0) d\mathbf{x}_0 dt_0. \quad (5)$$

$P(\mathbf{x}, t | \mathbf{x}_0, t_0)$ defines the probability of an air parcel released at time t_0 from a position \mathbf{x}_0 being observed at time t and position \mathbf{x} . The main challenge in Lagrangian dispersion modelling is to specify the transition probability. The most common approach solving the problem are stochastic Lagrangian models of turbulent diffusion. These particle trajectory simulations based on random-walk modelling were summarised by Rodean (1996). An alternative approach is the model of Raupach, which approximates the Lagrangian nature of turbulent dispersion analytically.

In the approach the velocity statistics in the canopy are used to specify the transition probability. The relation between $P(z, t | z_0, t_0)$ and the velocity statistics was first carried out by Taylor (1921). According to Raupach (1989a) and Seinfeld and Pandis (1998) the transition probability for a scalar released in a flow where the velocity is a stationary, Gaussian random process is itself Gaussian distributed.

$$P(z, t | 0, 0) = \frac{1}{\sigma_z(t)\sqrt{2\pi}} \exp\left(-\frac{z^2}{2\sigma_z^2(t)}\right). \quad (6)$$

For this supposed steady, homogeneous turbulence the vertical Lagrangian velocity and the vertical Eulerian velocity are equal and constant (Raupach, 1988) and the deviations of the velocities can be related by the kinematic theorem of Taylor (1921). This provides that the Eulerian vertical velocity standard deviation σ_w and the Lagrangian time scale T_L are known. This is very important due to the fact that only Eulerian turbulence statistics are directly measurable. The functional relationship between the Lagrangian and Eulerian vertical velocity variance is given by

$$\sigma_z^2(t) = 2\sigma_w^2 T_L^2 \left(\frac{t}{T_L} - 1 + \exp\left(-\frac{t}{T_L}\right) \right). \quad (7)$$

According to the theorem of Taylor (1921) Raupach identified two modes for the vertical velocity variance. In the so-called near-field condition $\sigma_z(t) \rightarrow \sigma_w t$ holds true if $t/T_L \rightarrow 0$. In the far-field mode, where $t/T_L \rightarrow \infty$ approaches infinity, $\sigma_z(t)$ equals $\sqrt{2\sigma_w^2 T_L(t - T_L)}$. This is the foundation for Raupach's (1989a) analytical approximation of the Lagrangian theory for the use

within and above canopies, which he termed the LNF Lagrangian theory.

Pollen can be considered as being emitted from a large number of point sources, the panicles of the maize plants. The spread of the fluid particles depends on the travel time. In the so-called near-field region, in which the travel time is less than the Lagrangian time scale $t \ll T_L$ and where the dispersion is dominated by persistence the particle trajectories depart little from straight lines. In the far-field region in which the travel time is longer $t \gg T_L$ the dispersion becomes diffusive. The scalar plume emitted from each panicle consequently passes through both the near- and far-field dispersion regimes, so that the overall scalar contribution in the canopy is at any point a superposition of contributions from plumes at all stages.

For this reason two cases of different diffusion regimes are considered for the specification of the transition probability, based on two assumptions of Raupach (1989a). The first assumption is that for long travel times $t - t_0$ the transition probability $P(z, t | z_0, t_0)$ for each source point (z_0, t_0) becomes a diffusion transition probability P_f which satisfies the diffusion equation with a characteristic far-field eddy diffusivity K_f . The second assumption describes the behaviour of the transition probability for travel times within the Lagrangian time-scale. For this non-diffusive, near-field part the Raupach approach submits a near-field transition probability P_n which can be approximated by the value in locally homogeneous turbulence, with velocity and time-scales $\sigma_w(z_0)$ and $T_L(z_0)$. In the near-field case

$$\frac{t - t_0}{T_L(z_0)} \rightarrow 0 \text{ leads to } P(z, t | z_0, t_0) \rightarrow P_n(z, t | z_0, t_0) \quad (8a)$$

and for the far-field case

$$\frac{t - t_0}{T_L(z_0)} \rightarrow \infty \text{ leads to } P(z, t | z_0, t_0) \rightarrow P_f(z, t | z_0, t_0 + T_L(z_0)). \quad (8b)$$

Applying these assumptions to the mean concentration yields an also decomposed concentration equation:

$$C(z) = C_n(z) + C_f(z), \quad (9)$$

$$C_n(z, t) = \int_0^\infty S(z_0) \int_0^t P_n(z, t | z_0, t_0) dz_0 dt_0. \quad (10)$$

This near-field term C_n is only significant for short travelling times and gets rather small for long times, so that sources beyond this short time contribute only to C_f . Applying the approach for the far-field part the integration limits have to be changed taking into account that the particle trajectories become diffusive when the travelling time extends more than the

Lagrangian time-scale.

$$C_f(z, t) = \int_0^\infty S(z_0) \int_0^{t - T_L(z_0)} P_f(z, t | z_0, t_0 + T_L(z_0)) dz_0 dt_0 \quad (11)$$

For the respective near- and far-field contribution analytical solutions must be found.

3.3.2. Non-diffusive near-field contribution C_n in homogeneous turbulence

Raupach defines an analytical near-field kernel function, which approximates the behaviour of the marked fluid particles for short travelling times. Advection is considered with restriction to variation in the stream-wise direction x . As C_n is significant for small travel times only, it is independent from \bar{u} . Under the condition that the value for inhomogeneous conditions can be approximated by its value for homogeneous conditions the non-advective case can be extended to advective conditions.

$$C_n(x, z) = \int_0^\infty \frac{S(x, z_0)}{\sigma_w(z_0)} \left(k_n \left(\frac{z - z_0}{\sigma_w(z_0) T_L(z_0)} \right) - k_n \left(\frac{z + z_0}{\sigma_w(z_0) T_L(z_0)} \right) \right) dz_0 \quad (12)$$

with the kernel function k_n . The second part of the kernel function accounts for the flow at the lower boundary $z = 0$ of the canopy. Due to the fact that the ground surface is a perfect absorber the concentration of the pollen at the ground is zero.

$$k_n(\zeta) = -0.39894 \ln(1 - e^{-|\zeta|}) - 0.15623e^{-|\zeta|}, \quad (13)$$

where ζ is the dimensionless distance with $\zeta = \frac{(z - z_0)}{\sigma_w T_L}$.

3.3.3. Diffusive far-field contribution C_f in inhomogeneous turbulence

The diffusive part C_f of C can be noted down directly for the advective case using the theoretical conclusions made before. Unlike to the situation in the near-field part, the persistence of the turbulence in the far-field part of a source can be assumed to have smaller length scales than the changes in the mean concentration gradient are and therefore gradient-diffusion theory can be applied. For advective conditions in the mean streamwise direction x the far-field concentration is given by the advection-diffusion equation (1) in stationary form with the modified source density $S_f(x, z)$ depending on height z and distance x . To conserve mass this modification of the source density is necessary, when the near-field concentration is included in the computations.

$$S_f(x, z) = \begin{cases} S(x, z) & \text{if } x > \bar{u}(0, z) T_L(0, z), \\ 0 & \text{else.} \end{cases} \quad (14)$$

For the far-field diffusivity K_f Raupach (1989a, b) formulates a term in dependence on the Eulerian vertical velocity standard deviation σ_w and the Lagrangian time scale T_L .

$$K_f(z, t) = \sigma_w^2(z, t)T_L(z, t). \tag{15}$$

An analytical solution for Eq. (1) and thus for the description of the diffusion process in the far field can be found when the turbulence structure is chosen practically. An analytical solution is available for a power-law turbulence.

$$\begin{aligned} \bar{u}(z_0) &= \bar{u}(h)\left(\frac{z_0}{h}\right)^\alpha, & \sigma_w(z_0) &= \sigma_w(h)\left(\frac{z_0}{h}\right)^{\beta_1}, \\ T_L(z_0) &= T_L(h)\left(\frac{z_0}{h}\right)^{\beta_2}. \end{aligned} \tag{16}$$

The power-law turbulence terms in Eq. (16) are specified by the turbulence situation at the top h of the canopy. According to Raupach (1989b) the values for the turbulence can be given by direct measurable values by $\bar{u}(h) = 3u_*(h)$, $\sigma_w(h) = 1.25u_*(h)$, $T_L(h) = 0.3h/u_*(h)$ where $u_*(h)$ denotes the friction velocity in height h . For the variables α and β Raupach proposed two values for α , one for sheared $\alpha = 1$ and one for unsheared flow $\alpha = 0$, when the velocity becomes a constant.

For the variable β Raupach (1989b) recommended three possible values $\beta_1 = \beta_2 = 0$, $\beta_1 = \beta_2 = 1/3$, $\beta_1 = \beta_2 = 1/2$ defining $\beta = 2\beta_1 + \beta_2$. The solution of Eq. (1) can be written in terms of a Green's function using this power-law turbulence structure

$$\begin{aligned} C_1(x, z|x_0, z_0) &= \frac{\mu}{z_0\bar{u}(z_0)\xi} \sqrt{\left(\frac{z}{z_0}\right)^{1-\beta}} \\ &\times \exp\left[-\frac{1}{\xi}\left(\left(\frac{z}{z_0}\right)^\mu + 1\right)\right] I_\nu\left[\frac{2}{\xi}\sqrt{\left(\frac{z}{z_0}\right)^\mu}\right]. \end{aligned} \tag{17}$$

I_ν is the modified Bessel function also known as hyperbolic Bessel function of order ν . The variables ν and μ are expressed by the variables α and β using

$$\begin{aligned} \mu &= \alpha - \beta + 2, \\ \nu &= (\beta - 1)/\mu. \end{aligned} \tag{18}$$

ξ is a function of x, x_0, z_0 and for K_f Eq. (15) is used.

$$\xi(x, x_0, z_0) = \left(\frac{K_f(z_0)}{z_0\bar{u}(z_0)}\right) \frac{\mu^2(x - x_0)}{z_0}. \tag{19}$$

With this function $C_1(x, z|x_0, z_0)$ for the transition probability in the Lagrangian approach the final form of the far-field concentration C_f for advective conditions is

$$C_f(x, z) = \int_0^x \int_0^z C_1(x, z|x_0, z_0)S_f(x_0, z_0) dx_0 dz_0. \tag{20}$$

Together with Eq. (12) it yields

$$C(x, z) = C_n(x, z) + C_f(x, z). \tag{21}$$

3.3.4. Modifications to the LNF approach

An application of the LNF theory to the underlying experimental design necessitates extensions. These modifications concern the deposition of particles, diverging of particles in directions other than the prevailing direction of wind and a variable source term.

The spatial domain of the given set of equations derived from LNF theory is the height z and the direction of prevailing wind x . Giddings (2000) introduces a weighting function, that may extend models of this type to incorporate different wind directions. The distribution of the weighting factor meets the fact that pollen dispersal in further distances can be observed in the field parts averted from wind as well. A modification of Giddings weighting factor w is

$$w(o) = \exp\left(-\frac{(o - \omega)^2}{f_w\sigma^2}\right). \tag{22}$$

It depends on the mean wind direction $\omega = 276^\circ$, the standard deviation $\sigma = 54^\circ$ and the orientation o of the sampling array. These parameter values are derived from the observed meteorological data of the experiment. The value of the parameter f_w describes how strong the dispersion is diminished in a single orientation. Giddings (2000) used $f_w = 2$ in his work. The comparison of the cross-pollination rates in the cardinal points for different values of f_w between 1 and 10 with the observed values shows that a value $f_w = 5$ yields a quite good fit to observed data. Particularly for the far-field concentration the wind and its direction play a decisive role. Due to this only the far-field contribution C_f is modified by the weighting factor.

Second, deposition plays an important role when observing the dispersion of heavy airborne particles like maize pollen. Raupach considered particles with negligible weight like CO_2 , heat and water vapour for which deposition rate of particles has been ignored in his studies. A constant deposition velocity is assumed for the calculation of the deposition rate of the pollen in the near- and far-field part. Di-Giovanni and Beckett (1990) discuss the uncertainties associated with the use of a constant deposition velocity. According to Emberlin et al. (1999) a constant deposition coefficient of $d = 0.2$ for maize pollen is used. Together with Eq. (21) this results in

$$\begin{aligned} C(x, z) &= C_n(x, z) + wC_f(x, z) \\ &- dC_n(x, z) - wdC_f(x, z). \end{aligned} \tag{23}$$

According to Raynor et al. (1972) the deposition per unit area at 60 m downwind is only 0.2% of that near the source. Considering this different deposition coefficients have to be used for the near- and far-field part.

Table 1
Overview of state variables and parameters

	Gaussian plume model		LNF theory model	
State variable	$C(x, y)$	mean concentration (kg m^{-3})	$C_n(x, y)$	near-field concentration (kg m^{-3})
	$P(x, y)$	Cross-pollination probability (%)	$C_f(x, y)$	far-field concentration (kg m^{-3})
Parameter			$P(x, y)$	Cross-pollination probability (%)
	K_1	eddy diffusivity for near distribution ($\text{m}^2 \text{s}^{-1}$)	$S(x_0, y_0)$	source density ($\text{kg m}^{-3} \text{s}^{-1}$)
	K_2	eddy diffusivity for far distribution ($\text{m}^2 \text{s}^{-1}$)	$u_*(h)$	friction velocity (m s^{-1}) at height h
	u_x	mean wind velocity in x direction (m s^{-1})	α	coefficient for description of \bar{u}
	u_y	mean wind velocity in y direction (m s^{-1})	β_1, β_2	coefficients for description of T_L and σ_w
	α_w	weighting factor for near and far distribution	w	weighting factor for wind direction
	t	time (s)	d	deposition coefficient
		h	average height of maize plants (m)	

A comparison with the field data show that a higher deposition coefficient in the near-field yields no better simulation results for the major part of the field. This shows that the observations of Raynor might be correct for the observed data in windward direction, but not for the entire field. For this reason for the near- and far-field part the same deposition coefficient of 0.2 is used for computation.

Third, in accordance to the experimental data for the source term a Gaussian distribution in height of the maize panicles is chosen.

$$S(x_0, x_s, z_0, z_s) = \exp\left(-\frac{(x_0 - x_s)^2}{p_1 h} - \frac{(z_0 - z_s)^2}{p_2 h}\right) \quad (24)$$

with x_s and z_s the location points of the panicles and p_1 , p_2 shape parameters of the source density. For reason of simplification it is assumed that the middle height of the panicles $z_s = 2.3$ m for all plants is the same and corresponds with the average measured height in the field experiment. The maize plants in the field experiment were planted at a distance of 0.75 m between the rows. This distance is used for calculation of x_s .

3.4. Estimation of cross-pollination probability

Denoting $C_{transgen}$ the amount of pollen a plant receives from all plants of the GM maize plot and C_{total} the sum of pollen a plant receives from all plants of the GM maize and all other non-GM maize plots the cross-pollination percentage P_{trans} can be described as

$$P_{trans} = \frac{C_{transgen}}{C_{total}}. \quad (25)$$

The underlying assumption of this approach is, that self-pollination of maize is negligible.

3.5. Model analysis

Before studying the results of the model application to the field experiment, the general behaviour and

properties of both models are to be derived. This will help to identify model parameters and to assess model output. As the described model is complex, highly nonlinear and not treatable analytically we use the methodology of sensitivity analysis, e.g. systematically varying of parameters, for studying system behaviour.

3.5.1. Sensitivity of Gaussian plume model

In the sensitivity analysis for both models the influence of the parameter values on the sum of deviation squares SQR^1 is analysed. In Table 1 the modelling parameters to be identified are listed. First can be preconceived that the parameter value of K_1 can be changed with that of K_2 , when the value of α_w is substituted to $1 - \alpha_w$. For values of α_w close to one the eddy diffusivity K_1 has for most of the simulation runs a well-defined minimum for the sum of deviation squares.

The sensitivity analysis yields that the values for parameter K_1 must be smaller than $5 \text{ m}^2 \text{ s}^{-1}$ and mostly even smaller than $1 \text{ m}^2 \text{ s}^{-1}$. This gives a small steep distribution form of the Gaussian graph. The parameter value of K_2 must first exceed a minimum value between 1 and $10 \text{ m}^2 \text{ s}^{-1}$. After the sharp decline of the SQR -value in this range SQR can hardly be minimised by increasing the values for K_2 . This results mostly in a weak local minimum for K_2 , but the form of the Gaussian graph is a wide shallow distribution for all. For all model runs the value of the eddy diffusivity K_1 is smaller than that for K_2 , which matches with the association of the physical process well.

The resulting SQR -values derived from the sensitivity analysis based on modified wind velocities u_x and u_y strongly depend on the accordance between the wind direction and the orientation of the sampling array. For a sampling array in x direction the influence of the wind velocity u_y is weak and vice versa. The parameter time t shows high correlation with the coefficients K_1 , K_2 ,

¹ SQR , sum of deviation squares of simulated and measured data (Richter and Söndgerath, 1990).

Table 2

Results of parameter estimation of sampling arrays in the cardinal points of the proving grounds and of sampling transections through the cardinal points

Array	C	G	L	P	C, L	G, P	C, G, L, P
$K_1(\text{m}^2 \text{s}^{-1})$	0.08	8.80	1.45	0.10	0.75	0.06	0.23
$K_2(\text{m}^2 \text{s}^{-1})$	5.51	65.01	55.30	77.46	75.73	37.14	16.40
$u_x(\text{m s}^{-1})$	-0.22	11.80	-0.13	6.63	0.33	1.69	0.37
$u_y(\text{m s}^{-1})$	3.53	-2.07	-1.44	-0.30	-1.43	-0.29	0.06
α_w	0.96	0.88	0.72	0.82	0.83	0.86	0.66
t (s)	4.75	4.75	4.75	4.75	4.75	4.75	4.75
<i>SQR</i>	0.003	0.04	0.16	0.12	0.36	0.19	0.95
r	1.00	0.99	0.96	0.98	0.97	0.92	0.97
<i>EF</i>	0.98	0.99	0.90	0.94	0.75	0.83	0.92

which is due to the multiplicative approach in Eq. (2). For this reason a fixed value for t was assumed.

3.5.2. Sensitivity LNF theory model

In the sensitivity analysis for the LNF theory model the influence of turbulence and wind profile specifying parameters is discussed. The values for the parameters $u_*(h)$, w , d and h can be deduced from field data and are not further examined.

The variables β_1 and β_2 affect the profiles of σ_w and T_L . For $\beta_1 = \beta_2 = 0$ a homogeneous turbulence is represented, the other two ($\beta_1 = \beta_2 = 1/2$, $\beta_1 = \beta_2 = 1/3$) represent levels of inhomogeneity characteristic of the adiabatic atmospheric surface layer and of canopy turbulence (Raupach, 1989b). Changing the turbulence type does not influence the near-field part, although the turbulence terms are included in Eq. (12). This is precisely what is supposed by the LNF theory: the turbulence situation is homogeneous for the near field. In the far field different parameter sets of β_1 and β_2 are only significant in proximity to the source. The highest inhomogeneity yields the highest concentration. This can be explained by the fact that in a situation in which advection occurs the turbulence can force the dispersing of particles. In an advective canopy the homogeneity ($\alpha = 0$) or inhomogeneity ($\alpha = 1$) of the wind profile specifies more than the turbulence terms. In a wind profile with unsheared flow in the far field the maximum concentration is only about a third of that with sheared flow.

4. Results

4.1. Parameter estimation within Gaussian plume model

Parameter estimation denotes the mathematical procedure of identification the set of model parameters that leads to a simulation trajectory with a minimum deviation to the measured cross-pollination rates

(Richter and Söndgerath, 1990). These algorithms additionally support a statistical analysis of the correlation between the model parameters as well as estimates on the standard deviation of the model parameters. For this it is necessary to calculate partial derivative of the SQR-values with respect to the unknown model parameters. As these are difficult to calculate, we use a simple but robust gradient-free minimum search for parameter estimation.² Thus, the discussion of the parameter estimation bases with respect to parameter correlation and the identification of local or global minima on the results obtained from the sensitivity analysis.

Based on the experimental results from 1 year, model performance cannot be assessed with respect of transferability to different sites and climatic conditions (years). The first important step is to analyse, if the model is capable of reproducing the observed pattern of the investigation site focussing on the independent variables of wind direction and transect. The appropriate methodology for those cases is to separate the available data set into a “training” and “test” data set, using the training-data set for parameter estimation than applying the model to the test data set.

First, parameter identification is performed for single sampling arrays in the cardinal points of the proving grounds (array C, G, L, P; cf. Table 2). Per definition the wind in y direction blowing southward gets a negative sign. The *EF* values³ for the modelling efficiency and the correlation coefficient r show that the optimisation results are quite satisfying.

In terms of testing the validity of the model we focus on the question of whether the parameter set of a main orientation can be used to predict the observed data arrays for other wind directions. For this aim the

² FindMinimum-Procedure in the symbolic mathematics package Mathematica[®] 4.1.

³ The modelling efficiency (EF) has the maximum value 1 for the best fit, the predicted values describe the observed values exactly. If *EF* is less than zero the model-predicted values are worse than simply using the observed mean (Loague and Green, 1991).

Table 3

Statistical criteria of goodness of fit—parameter sets of the cardinal points are transferred to other arrays in the same orientation

Array	Fit with parameter set of C		Fit with parameter set of G	
	B	D	F	H
<i>r</i>	0.99	0.92	0.90	0.94
<i>EF</i>	0.70	0.40	−0.64	−4.95

Array	Fit with parameter set of L		Fit with parameter set of P	
	K	M	O	Q
<i>r</i>	0.99	0.99	0.93	0.80
<i>EF</i>	0.77	0.97	0.68	−0.48

parameter derived from a array of a cardinal point are used to test the model output at the neighbored arrays, e.g. set of array C is applied to arrays B and D. The results show that the model is able to predict cross-pollination rates of test data with the parameters sets found by training data, especially for those arrays that belong to the leeward (array C) and windward directions (array L), cf. Table 3.

Next we consider two arrays for parameter estimation to study, if the derived single parameter set is capable of simulating the data for the entire field. Parameters are identified for a transection in the west–east (row C and L) and a transection in the north–south (row G and P) orientation and both transections are evaluated in one step as well and then used for the simulation of data for the entire field, cf. Table 2. Finally the sampling arrays for the entire field are used for parameter estimation, cf. Table 4.

The parameter ranges are summarised in Table 4 and compared with the result of the optimisation for the entire field. To reach more consistency in the parameter range the value for K_1 in array G is not taken into account. Further it must be considered that for the wind velocity u_x only the values from the relevant sampling arrays (C; L; C and L; C, G, L, P) are taken. The same applies to u_y . All parameters lie in reasonable ranges, which means that they show consistency with the observed field data.

4.2. Parameter identification for LNF theory model

In the LNF theory approach most of the parameter values are given by physical measurements. For this reason parameter estimation is omitted. Only a few single changes of the turbulence parameters and the source density are investigated. The effect of these changes on the cross-pollination rate are discussed and compared by measures of goodness of fit in this section.

First the consequence of different source strengths is studied. As an example source densities $S_l(x_0, z_0)$ (large), $S(x_0, z_0)$ and $S_s(x_0, z_0)$ (small) of Gaussian shape with $p_1 = 2.0, 1.0$ and 0.5 and $p_2 = 0.4, 0.2$ and 0.1 are

Table 4

Combined results of parameter optimisation of sampling arrays listed in Table 2 and result of parameter optimisation of the entire field with *FindMinimum* search

Parameter	Range of values	All
$K_1(\text{m}^2 \text{s}^{-1})$	0.06–1.45	1.08
$K_2(\text{m}^2 \text{s}^{-1})$	5.51–75.73	149.44
$u_x(\text{m s}^{-1})$	−0.13–0.37	0.93
$u_y(\text{m s}^{-1})$	−2.07–0.06	0.11
α_w	0.66–0.96	0.63
t (s)	4.75	1.66
<i>r</i>	0.92–1.00	0.90
<i>EF</i>	0.75–0.99	0.66

studied, cf. Eq. (24). As expected a higher concentration profile results for the stronger source strengths in both fields and vice versa. In the near field the concentration increases in the same proportion as the source strength does. For a source $S_s(x_0, z_0)$ with a strength half of $S(x_0, z_0)$ the concentration C_{ns} is also about half as low than C_n and the same applies to C_{nl} . In the far field both the point of the highest concentration and the proportion between resulting concentration and source strength are displaced. Doubling the source strength increases the concentration higher than twice.

Array N is chosen to examine the effect of the source strength on the cross-pollination rate. The resulting model efficiency values are $EF = 0.62$ for $S(x_0, z_0)$, $−59.74$ and $−0.62$, for $S_l(x_0, z_0)$ and $S_s(x_0, z_0)$. This shows that the greater source S_l leads to an over-estimation of the cross-pollination rate and the smaller source S_s undervalues the rate. Based on this the parameters of the source function are set to $p_1 = 1$ and $p_2 = 0.2$.

The problem in the fit of the field data is that the sharp decline of the cross-pollination rate between near- and far-field parts must be rendered. This decline is especially influenced by the choice of the values for β_1 and β_2 . Parameter α is most responsible for the height of the cross-pollination rate. For $\beta_1 = \beta_2 = 0$ the smoothest and for $\beta_1 = \beta_2 = \frac{1}{2}$ the deepest decline can be

observed. Due to this the $\alpha = 1$ and $\beta_1 = \beta_2 = \frac{1}{2}$ is set for all further computations.

The friction velocity u_* must be deduced from the observed mean wind velocity at the top of the canopy. This is derived by the wind profile of the maize canopy. Furthermore, the scalar transfer in a canopy depends on the momentum transfer and the structure of the turbulent wind field. Detailed models for the simulation of airflow within and above vegetative environments have been developed in many works, see for instance Shaw et al. (1974), Raupach and Thom (1981), Wilson and Shaw (1977), Meyers and Paw (1986), Miller et al. (1991) for full model descriptions. We refer to the approach from Raupach and Thom (1981) in the following. With this approach for the observed wind velocity of $u(h) = 1.13 \text{ m s}^{-1}$ a friction velocity of $u_*(h) = 0.36 \text{ m s}^{-1}$ results (calculated with a roughness length z_0 of 0.26 m, a zero-plane displacement height d_0 of 1.53 m and an effective drag coefficient C_d of 0.2). In Fig. 2 the simulated wind profile is represented graphically. With this final assumption all the parameters needed for computation are determined and summarised in Table 5.

4.3. Modelling results

4.3.1. Spatially explicit simulation Gaussian plume model

In the approach with the Gaussian plume model an almost accurate simulation of the observed data can be

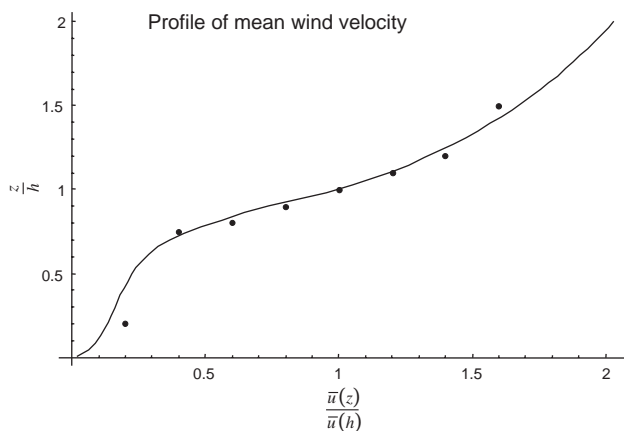


Fig. 2. Profile of mean wind velocity in a maize canopy ($h = 2.45 \text{ m}$) with a measured mean wind velocity at the top of $\bar{u}(h) = 1.13 \text{ m s}^{-1}$; plot points = corresponding reference values measured in a maize canopy ($h = 2.1 \text{ m}$) during periods of light wind ($\bar{u}(h) = 0.88 \text{ m s}^{-1}$) published by Raupach and Thom (1981).

reached for single sample arrays as obvious from the statistical measures (cf. Table 2). If the data sets of parameter estimation are extended the goodness of fit is still high. As an example the simulation of the cross-section in west–east direction (main direction of wind) is presented graphically in Fig. 3. The high cross-pollination percentages at the edge of the GM maize field are the weak point in the calculation. The observed percentages at distances of 3 and 4.5 m from the edge are overestimated for the windward as well as for the leeward part of the field. This can be explained by the simplification to one eddy diffusivity for both wind directions in the model. The natural process in fact is more complex. In the model the different cross-pollination percentages result from the influence of the wind velocity only. For the cross-pollination percentages in longer distances from the edge of the GM maize field the simulation gets more precise and only a slight trend to underestimation in the windward part is observable.

4.3.2. Spatially explicit simulation LNF theory model

A cross-section through the main leeward and windward-sampling array is presented in Fig. 4. The figure shows that the model can simulate the cross-pollination rates for longer distances quite well, although a few data are slightly overestimated. The data in immediate proximity to the edge of the GM maize field are undervalued by the model. In the leeward direction the undervaluation lies in a range of about 0.8%. In the windward direction the high cross-pollination rate at immediate edge of the GM maize field (3 m distance) is underestimated by the model in a range of about 17%. The cross-pollination rate at a distance of 4.5 m accords with the observed data more. In the values for the modelling efficiency ($EF = 0.340$) and the correlation coefficient ($r = 0.874$) the suitability of the model is reflected.

The graphical display shows that the sharp decline of the cross-pollination rate is predicted to be closer to the edge of the GM maize field. Applying LNF theory decline of the cross-pollination rate can be explained by the termination of influence of the near-field part of the transgenic plants.

4.4. Model comparison

For a comparison of both modelling approaches two figures are compiled, which display the spatially explicit cross-pollination probabilities. Fig. 5 displays the cross-

Table 5

Results of the parameter optimisation for the LNF theory model without an automatic minimisation algorithm

Parameter	α	$\beta_1 = \beta_2$	$S(x_0, z_0)$	f_w	d	h (m)	$u_*(h)$ (m s ⁻¹)
Value	1	0.5	$p_1 = 1, p_2 = 0.2$	5	0.2	2.45	0.36

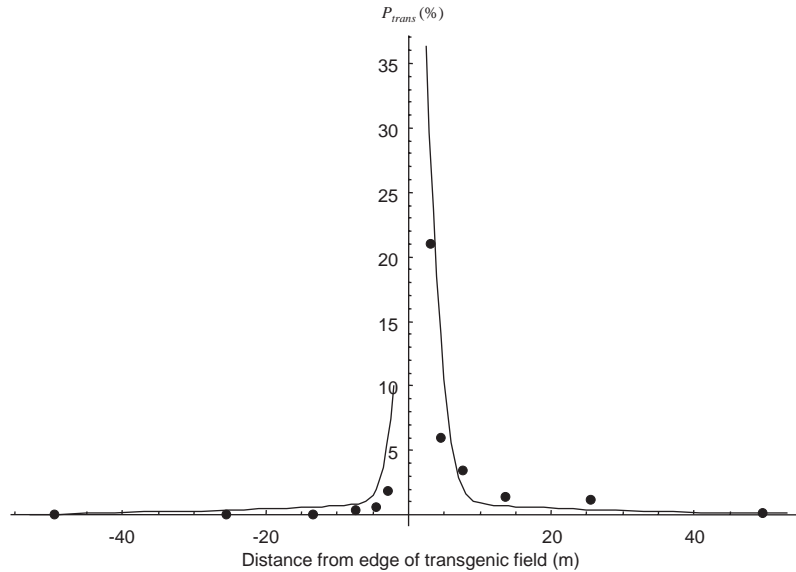


Fig. 3. Gaussian plume model—simulation of cross-section in west-east direction (array C—left and L—right) with FindMinimum tool ($K_1 = 0.747 \text{ m}^2 \text{ s}^{-1}$, $K_2 = 75.730 \text{ m}^2 \text{ s}^{-1}$, $u_x = 0.327 \text{ m s}^{-1}$, $u_y = -1.431 \text{ m s}^{-1}$, $\alpha_w = 0.833$, $t = 4.75 \text{ s}$), plot points = observed data.

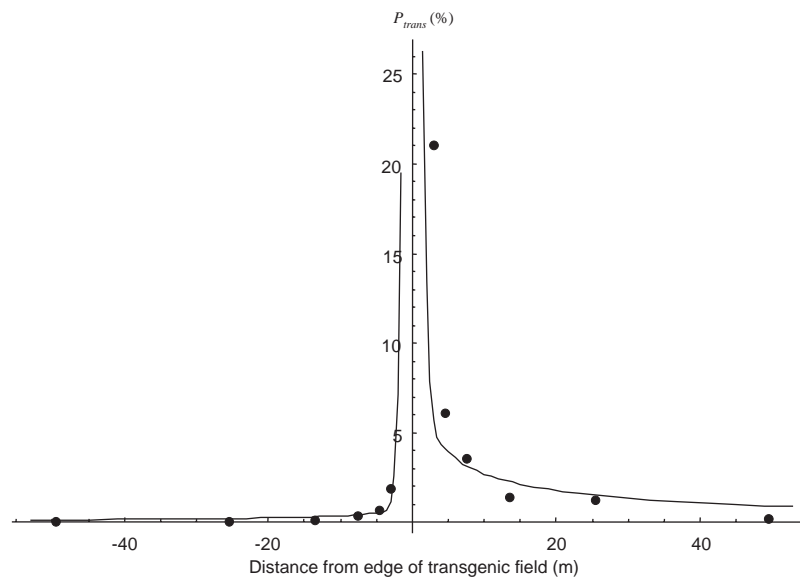


Fig. 4. LNF theory model—simulation of cross-section in west-east direction (array C—left and L—right) ($\alpha = 1$, $\beta_1 = \beta_2 = \frac{1}{2}$, $u_*(h) = 0.36 \text{ m s}^{-1}$, $d = 0.2$, $f_w = 5$), plot points = observed data.

pollination probability derived from a simulation using the Gaussian plume model (upper left) and the model based on LNF theory (upper right). The absolute deviations from the observed values are displayed in the lower figures.

Fig. 6 shows scatter diagrams of values from the Gaussian plume model and LNF theory approach for orientation west (array A, B, C, D, E), north (array E, F, G, H, I), east (array I, K, L, M, N), south (array N, O, P, Q, A).

For both models a clear symmetrical distribution of the values is given (cf. Fig. 5). The Gaussian plume

model yields a clear square form with accentuation at the main orientations and irruption at the corners. These irruption at the corners leads to great deviations from the measured data for corner I and N and correct predictions for A and E. It is striking that this pattern appears in the observed data as well as in the model-predicted data in the part averted from the wind. This pattern may be explained by the field geometry and by the method after which the maize rows are planted. Especially in the corners the diffusion process is non-isotropic. Note, turbulent diffusion process is assumed to be independent from direction in Eq. (3), which

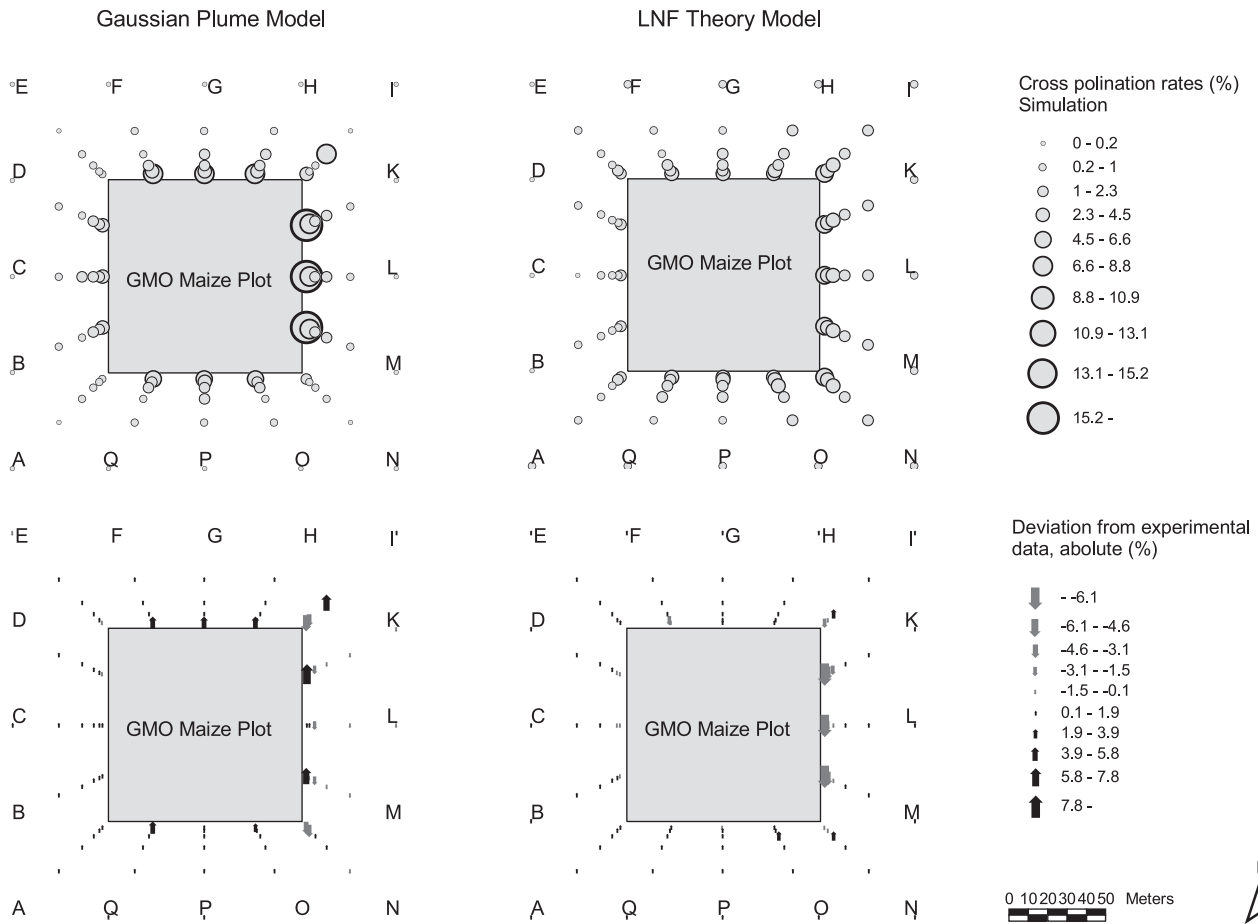


Fig. 5. Comparison of the simulation with the Gaussian plume model (left, $K_1 = 1.076 \text{ m}^2 \text{ s}^{-1}$, $K_2 = 149.439 \text{ m}^2 \text{ s}^{-1}$, $u_x = 0.926 \text{ m s}^{-1}$, $u_y = 0.108 \text{ m s}^{-1}$, $\alpha_w = 0.632$, $t = 1.660 \text{ s}$) with that of the LNF theory model (right, $\alpha = 1$, $\beta_1 = \beta_2 = \frac{1}{2}$, $u_*(h) = 0.36 \text{ m s}^{-1}$, $d = 0.2$) and absolute deviations from observed field data.

implicitly assumes isotropy. Another striking result is the high-predicted rate in row I at a distance of 13.5 m. This high rate is also found in the measured data. However, the model overestimates the value by about 6%.

The results of the simulation based on LNF theory are dominated by the weighting factor, which expresses the influence of the wind, cf. Section 3.3.4. Due to the assumed symmetry using the exponential function no irregularities in the corners of the field occur, which then result in an overestimation of the field data in corner A and E and a correct prediction for corner I and N.

For a detailed analysis of the model goodness, one scatter diagram for each cardinal point is necessary, in which the observed values are plotted on the x -axis and the model-predicted values on the y -axis, cf. Fig. 6. In the West cross-pollination data shows small ranges. It can be pointed out, that in both models the values in longer distances from the GM maize field are overestimated. In the LNF theory there is additionally a slight underestimation at the edge of the field. But the deviations in the leeward direction are comparatively small.

In the north both models can simulate the field data very precisely. A slight trend to an overestimation is found for both in the data for further distances. A systematic deviation can be observed for the Gaussian plume model at a distance of 3 m. The model predicts higher rates than the observed ones actually are. This can be explained by the optimised parameter value for the wind in north–south direction. With the small positive value a slight wind in north direction is assumed. In the North the average rates (including row I) observed in the field are higher, although the wind measurement in the field yields a slight orientation of the wind in the south. Such a discontinuity in the field measurement certainly leads to problems in the simulation result. Because in the LNF theory the cross-pollination rate is determined by the wind measurements the problem has no impact there.

In the scatter diagram for the east the weak point in the LNF theory model is obvious as discussed before. It is the simulation of the high cross-pollination rate at the edge of the GM maize field. But in the diagram one can also see that the Gaussian model overestimates the rate at a distance of 3 m for array K and M. For the sample

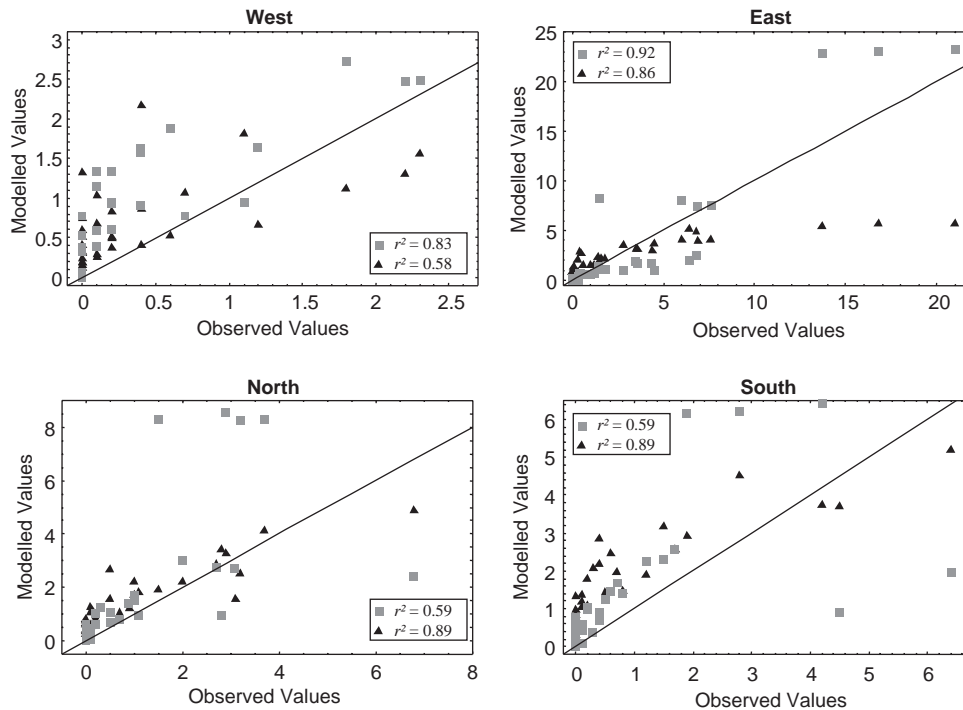


Fig. 6. Scatter diagram of values from the Gaussian plume model (\square) and LNF theory approach (\blacktriangle) for orientation west (array A, B, C, D, E), north (array E, F, G, H, I), east (array I, K, L, M, N), south (array N, O, P, Q, A). In general, the high values in the diagram represent the cross-pollination percentage at the edge of the GM maize field, the small ones those for the remoter area.

points in the middle part of the ordinary field (distance 7.5 m) the Gaussian model predicts a sharp decline conditioned by the end of the near-distribution influence. This part is simulated more precisely by the LNF theory, because the decrease of the rate is very smooth for all arrays and sharp bends like in the Gaussian model do not occur. But in turn, this leads to slightly increased percentages at the far end of the ordinary field in the LNF theory.

In the south the situation is similar to that in the north. The Gaussian model simulates some to high rates for the data at the edge of the GM maize field. In the LNF theory the weak point is the simulation in the remoter area with an overestimation of the cross-pollination percentage. An overestimation can be observed for the Gaussian plume model there too, although it is minor.

Summarised in statistical measures the result for the Gaussian plume model is a modelling efficiency of $EF = 0.664$ and a correlation coefficient of $r = 0.896$. Compared with that for the LNF theory with $EF = 0.562$ and $r = 0.827$ the simulation of the two approaches achieves approximately the same goodness of fit.

For both models it is difficult to simulate the small cross-pollination percentages in the parts far from the GM maize plot with the same high precision. The small percentages at the parts averted from the wind in west, north and south direction can be reproduced satisfyingly although often a slight overestimation is observable. The

higher percentages in wind direction can be predicted better like this. At the edge of the GM maize field the approach with the Gaussian plume model has an advantage in the parts against and in wind direction. But the simulation with the LNF theory is better in the north and south. None of the two approaches can gain a clear advantage in the simulation of the field data, but both can reproduce the observed values with deviations in a reasonable and acceptable range.

5. Conclusion

Both modelling approaches are appropriate for the simulation of the cross-pollination rates. The typical “bi-phasic” decent of cross-pollination rates are reproduced, and a physical explanation for this pattern is given. Furthermore, the obtained model results are spatially explicit and therefore allow an analysis of cross-pollination experiments depending on the field geometry. The advantage in the simulation with the LNF theory is that the smooth decrease of the cross-pollination rate with distance is only determined by the introduced physical measures and this yields results in good accordance with the field data.

Both approaches—Lagrangian and Eulerian—are equivalent under coordinate transformation. Both models (Gauss and LNF) are derived from analytical solutions of Eq. (1). However, both approaches differ

in several general topics. The Gaussian plume model is set up by a superposition of analytical solutions of Eq. (1). Parameters can be identified only by the application of parameter estimation procedures. This requires sufficient experimental data and makes it difficult to transfer the quantitative results to different investigation sites with other environmental conditions. However, the advantages of this approach are the small number of free parameters, the simplicity in defining different spatial configuration of the donor and recipient field and the less computational effort for this model.

The LNF theory model can be specified by physically measurable parameters. The number of free parameters is limited. This supports model applications at different investigation sites. However some model part (see Eq. (21)) are still empirical. Based on the simulation results and the model analysis we can identify further research demands:

1. A question still open is whether the rather small near-field contribution in Raupach's theory is equal to the situation in natural canopies. This question was analysed in the work of Van den Hurk and McNaughton (1995) and Katul et al. (1997) as well and must remain to be the object of further studies. Main focus is to be laid onto the introducing of the dependency on the direction of wind to LNF theory.
2. Import pattern not supported by both modelling approaches are non-isotropic conditions in the field, caused by the way maize is planted, see for instance results for arrays A, E, I, N. For these conditions two eddy diffusivities of the Gaussian plume model are to be substituted by a diffusivity tensor.
3. The retention of particles in plant canopies is a very complex process influenced by the local aerodynamics, the structure of the particles and the nature of the plant surfaces. Further research need to focus on the deposition of heavy particles. However, a low parametrisation of deposition defines a somehow worst case in terms of risk assessment of transgenic crops, as more pollen remains available for pollination.

In general, the developed modelling approaches are transferable and applicable to other crops as long as the air transport of pollen is considered. Further modelling effort has to be spent on biological issues, such as insect movement if insects play a role for pollination, viability of pollen and the dynamic aspects of flowering time of plants.

For further applications the topography of the investigation site has to be considered. Advection and wind profiles may change in space due to varying land use types, roughness parameters and thermal conditions.

The models offer a tool for analysis and assessment of cross-pollination experiments. Especially the LNF

theory model is applicable to real-world problems as most of the parameters can be specified by measurable variables. This allows a model-supported risk assessment and uncertainty analysis and the model-based identification of management strategies of GM crops and provides a basis for the ongoing discussion on thresholds for the adventitious presence of GM material in food and feed.

References

- Baldocchi, D., 1997. Flux footprints within and over forest canopies. *Boundary-Layer Meteorol.* 85, 273–297.
- DFG Senate commission, 2001. Threshold values for products from genetically modified plants: statement by the DFG Senate Commission for the assessment of chemicals used in agriculture. <http://www.dfg.de> [June, 2002].
- Di-Giovanni, F., Beckett, P.M., 1990. On the mathematical modelling of pollen dispersal and deposition. *J. Appl. Meteorol.* 29, 1352–1357.
- Emberlin, J., Adams-Groom, B., Tidmarsh, J., 1999. A report on the dispersal of maize pollen. <http://www.soilassociation.org> [September, 2001].
- Giddings, G., 2000. Modelling the spread of pollen from *Lolium perenne*: the implications for the release of wind-pollinated transgenics. *Theor. Appl. Genet.* 100, 971–974.
- Gu, L., Shugart, H.H., Fuentes, J.D., Black, T.A., Shewchuk, S.R., 1999. Micrometeorology, biophysical exchanges and NEE decomposition in a two-story boreal forest—development and test of an integrated model. *Agric. Forest Meteorol.* 94, 123–148.
- Katul, G., Oren, R., Ellsworth, D., Hsieh, C., Phillips, N., 1997. A Lagrangian dispersion model for predicting CO₂ sources, sinks and fluxes in a uniform loblolly pine (*Pinus taeda* L.) stand. *J. Geophysical Res.* 102, 9309–9321.
- Katul, G.G., Albertson, J.D., 1999. Modelling CO₂ sources, sinks and fluxes within a forest canopy. *J. Geophysical Res.* 104, 6081–6091.
- Lavigne, C., Klein, E.K., Vallée, P., Pierre, J., Godelle, B., Renard, M., 1998. A pollen-dispersal experiment with transgenic oilseed rape: estimation of the average pollen dispersal of an individual plant within a field. *Theor. Appl. Genet.* 96, 886–896.
- Loague, K., Green, R.E., 1991. Statistical and graphical methods for evaluating solute transport models: overview and application. *J. Contaminant Hydrol.* 7, 51–73.
- Massman, W.J., 1999. A model study of kB_h^{-1} for vegetated surfaces using 'localized near-field' Lagrangian theory. *J. Hydrol.* 223, 27–43.
- Meier-Bethke, S., Schiemann, J., 2000. Monitoring influences of plantation of GM crops to agro-ecosystems, Sub-project 1: cross pollination of GM corn in adjacent non-transgenic corn fields and qualification of transgenic contamination in harvest biomass. Annual Report (in German). <http://www.ptj-jahresbericht.de/archiv.html> [July, 2003].
- Meier-Bethke, S., Schiemann, J., 2002. Cross pollination of GM corn in adjacent non-transgenic corn fields. In: Proceedings of the 7th International Symposium on the Biosafety of Genetically Modified Organisms. Beijing, China, pp. 295.
- Meyers, T.P., Paw, K.T., 1986. Testing of a higher-order closure model for modeling airflow within and above plant canopies. *Boundary-Layer Meteorol.* 37, 297–311.
- Miller, D.R., Lin, J.D., Lu, Z.N., 1991. Air flow across an alpine forest clearing: a model and field measurements. *Agric. Forest Meteorol.* 56, 209–225.

- Raupach, M.R., 1987. A Lagrangian analysis of scalar transfer in vegetation canopies. *Quart. J. Roy. Meteorol. Soc.* 113, 107–120.
- Raupach, M.R., 1988. Canopy transport processes. In: Steffen, W.L., Denmead, O.T. (Eds.), *Transport in the Natural Environment: Advances and Applications*. Springer, Berlin, pp. 95–127.
- Raupach, M.R., 1989a. Applying Lagrangian fluid mechanics to infer scalar source distributions from concentration profiles in plant canopies. *Agric. Forest Meteorol.* 47, 85–108.
- Raupach, M.R., 1989b. A practical Lagrangian method for relating scalar concentrations to source distributions in vegetation canopies. *Quart. J. Roy. Meteorol. Soc.* 115, 609–632.
- Raupach, M.R., Thom, A.S., 1981. Turbulence in and above plant canopies. *Ann. Rev. Fluid Mech.* 13, 97–129.
- Raynor, G.S., Ogden, E.C., Hayes, J.V., 1972. Dispersion and deposition of corn pollen from experimental sources. *Agronomy J.* 64, 420–427.
- Richter, O., Söndgerath, D., 1990. *Parameter Estimation in Ecology*. VCH Publishers, Weinheim.
- Rodean, H.C., 1996. Stochastic Lagrangian models of turbulent diffusion. *Meteorol. Monographs* 26 (48), 82.
- Seinfeld, J.H., Pandis, S.N., 1998. *Atmospheric Chemistry and Physics: From Air Pollution to Climate Change*. Wiley, New York.
- Shaw, R.H., den Hartog, G., King, K.M., Thurtell, G.W., 1974. Measurements of mean wind flow and three-dimensional turbulence intensity within a mature corn canopy. *Agric. Forest Meteorol.* 13, 419–425.
- Taylor, G.I., 1921. Diffusion by continuous movements. *Proc. London Math. Soc. A* 20, 196–212.
- Treu, R., Emberlin, J., 2000. Pollen dispersal in the crops Maize (*Zea mays*), Oil seed rape (*Brassica napus ssp oleifera*), Potatoes (*Solanum tuberosum*), Sugar beet (*Beta vulgaris sp. vulgaris*) and Wheat. <http://www.soilassociation.org> [January 2002].
- Van den Hurk, B.J.J.M., McNaughton, K.G., 1995. Implementation of near-field dispersion in a simple two-layer surface resistance model. *J. Hydrol.* 166, 293–311.
- Warland, J.S., 1999. Applications and theory of micrometeorological flux measurement. Ph.D. Thesis, University of Guelph.
- Wilson, N.R., Shaw, R.H., 1977. A higher order closure model for canopy flow. *J. Appl. Meteorol.* 16, 1197–1205.